

Ultrafast magneto-optical dynamics in nickel (111) single crystal studied by the integration of ultrafast reflectivity and polarimetry probes

Hao Kuang(匡皓), Junxiao Yu(余军潇), Jie Chen(陈洁), H. E. Elsayed-Ali, Runze Li(李润泽), and Peter M. Rentzepis
Citation: Chin. Phys. B, 2024, 33 (**3**): 037802. DOI: 10.1088/1674-1056/ad1983
Journal homepage: http://cpb.iphy.ac.cn; http://iopscience.iop.org/cpb

What follows is a list of articles you may be interested in

Probing photocarrier dynamics of pressurized graphene using time-resolved terahertz spectroscopy

Yunfeng Wang(王云峰), Shujuan Xu(许淑娟), Jin Yang(杨金), and Fuhai Su(苏付海)
Chin. Phys. B, 2023, 32 (**6**): 067802. DOI: 10.1088/1674-1056/acc2b1

An ultrafast spectroscopy system for studying dynamic properties of superconductors under high pressure and low temperature conditions

Jian Zhu(朱健), Ye-Xi Li(李叶西), Deng-Man Feng(冯登满), De-Peng Su(苏德鹏), Dong-Niu Fan(范东牛),Song Yang(杨松), Chen-Xiao Zhao(赵辰晓), Gao-Yang Zhao(赵高扬), Liang Li(李亮),Fang-Fei Li(李芳菲), Ying-Hui Wang(王英惠), and Qiang Zhou(周强)
Chin. Phys. B, 2023, 32 (**6**): 067801. DOI: 10.1088/1674-1056/acc0f5

Ultrafast proton transfer dynamics of 2-(2'-hydroxyphenyl)benzoxazole dye in different solvents

Simei Sun(孙四梅), Song Zhang(张嵩), Jiao Song(宋娇), Xiaoshan Guo(郭小珊), Chao Jiang(江超), Jingyu Sun(孙静俞), and Saiyu Wang(王赛玉)
Chin. Phys. B, 2022, 31 (**2**): 027803. DOI: 10.1088/1674-1056/ac3734

Spectral polarization-encoding of broadband laser pulses by optical rotatory dispersion and its applications in spectral manipulation

Xiaowei Lu(陆小微), Congying Wang(王聪颖), Xuanke Zeng(曾选科), Jiahe Lin(林家和), Yi Cai(蔡懿), Qinggang Lin(林庆钢), Huangcheng Shangguan(上官煌城), Zhenkuan Chen(陈振宽), Shixiang Xu(徐世祥), and Jingzhen Li(李景镇)
Chin. Phys. B, 2021, 30 (**7**): 077801. DOI: 10.1088/1674-1056/abf0fb

Temperature dependent terahertz giant anisotropy and cycloidal spin wave modes in $BiFeO_3$ single crystal

Fan Liu(刘凡), Zuanming Jin(金钻明), Xiumei Liu(刘秀梅), Yuqing Fang(方雨青), Jiajia Guo(国家嘉), Yan Peng(彭滟), Zhenxiang Cheng(程振祥), Guohong Ma(马国宏), Yiming Zhu(朱亦鸣)
Chin. Phys. B, 2020, 29 (**7**): 077804. DOI: 10.1088/1674-1056/ab8dae

---

SPECIAL TOPIC — States and new effects in nonequilibrium

Ultrafast magneto-optical dynamics in nickel (111) single crystal studied by the integration of ultrafast reflectivity and polarimetry probes

Hao Kuang(匡皓)[1,2], Junxiao Yu(余军潇)[3], Jie Chen(陈洁)[3], H. E. Elsayed-Ali[4], Runze Li(李润泽)[1,2,†], and Peter M. Rentzepis[5,‡]

[1] *School of Physical Science and Technology, ShanghaiTech University, Shanghai* 201210, *China*
[2] *Center for Transformative Science, ShanghaiTech University, Shanghai* 201210, *China*
[3] *Center for Ultrafast Science and Technology, Key Laboratory for Laser Plasmas (Ministry of Education), Collaborative Innovation Center of IFSA (CICIFSA), School of Physics and Astronomy, Shanghai Jiao Tong University, Shanghai* 200240, *China*
[4] *Department of Electrical and Computer Engineering, Old Dominion University, Norfolk, Virginia* 23529, *USA*
[5] *Department of Electrical and Computer Engineering, Texas A&M University, College Station, Texas* 77843, *USA*

(Received 28 November 2023; revised manuscript received 27 December 2023; accepted manuscript online 29 December 2023)

With the integration of ultrafast reflectivity and polarimetry probes, we observed carrier relaxation and spin dynamics induced by ultrafast laser excitation of Ni (111) single crystals. The carrier relaxation time within the linear excitation range reveals that electron–phonon coupling and dissipation of photon energy into the bulk of the crystal take tens of picoseconds. On the other hand, the observed spin dynamics indicate a longer time of about 120 ps. To further understand how the lattice degree of freedom is coupled with these dynamics may require the integration of an ultrafast diffraction probe.

Keywords: ultrafast spin dynamics, non-equilibrium dynamics, multi-probe

PACS: 78.47.J–, 42.65.Re, 75.78.Jp **DOI:** 10.1088/1674-1056/ad1983

1. Introduction

In recent years, ultrafast demagnetization by photoexcitation has attracted pronounced research efforts due to its potential applications in next-generation ultrafast magnetic storage devices, magneto-optical devices, spintronics studies and others.[1] The ultrafast optical excitation of magnetic materials typically involves nonequilibrium relaxation dynamics among different degrees of freedom, including electron, spin, lattice and even orbital subsystems. For ferromagnetic metals, it is generally believed that irradiation of femtosecond optical pulses will create a nascent hot electron gas, and the Drude model is generally used to evaluate the metal's optical responses to such excitations.[2] The coupling of energies within the electronic subsystem into the spin or lattice subsystems subsequently induces transient change in magnetic order or the periodic arrangement of atoms. In the 1990s, it was demonstrated that the demagnetization of nickel single crystal subjected to femtosecond laser irradiation occurred within hundreds of femtoseconds,[3] a time scale that is much smaller than the spin–lattice interaction mechanism that is of the order of picoseconds. Similar observations were made in other ferromagnetic 3d transition metals, such as cobalt and iron, upon ultrafast photon excitations.[4–6] Therefore, an effective means for the evaluation of coupling dynamics among different degrees of freedom is to create nonequilibrium states with ultrafast pulses and observe the sequential relaxation processes leading to equilibrium states.[7–9] For example, recent experiments have reported Morin phase transitions, giant Kerr rotations, coherent spin-wave transport and spin-polarized gaps.[10–14] Despite those extensive studies on the time scale of couplings among different degrees of freedom, one outstanding question raised in the past few years is where does the spin angular momentum go during the ultrafast demagnetization process? The rapid development of ultrafast diffraction methods in recent years has shone a light on this question from an interesting perspective. For example, it has been proved in an iron thin film that the missing spin angular moment will transfer to the lattice to cause a shear motion in order to maintain the conservation of angular momentum.[5] This angular momentum transfer occurs within a time interval of picoseconds and is named the ultrafast Einstein–de Hass effect, a counterpart of the macroscopic classical Einstein–de Hass effect. A similar effect was observed in other ferromagnetic materials such as nickel,[15] and antiferromagnetic materials such as $FePS_3$.[16] Overall, the evolution of nonequilibrium dynamics associated with magnetic materials requires various experimental methods that are individually sensitive to the response of different degrees of freedom. For example,

†Corresponding author. E-mail: lirz@shanghaitech.edu.cn
‡Corresponding author. E-mail: prentzepis@tamu.edu

© 2024 Chinese Physical Society and IOP Publishing Ltd

the hot electron gas is typically probed through ultrafast optical reflectivity or transmission measurements; the spin angular momentum can be revealed by observing the transient change of optical polarizations, and the lattice structural dynamics require ultrafast diffractions using femtosecond electron or x-ray pulses that are generated either on laboratory size apparatus or large facilities. However, photon-induced nonequilibrium dynamics generally involve couplings among different degrees of freedom. The integration of ultrafast reflectivity, polarimetry and diffraction probes may provide a unified time frame for studying the same sample area under the same photon-excitation conditions.

Here, we employed ultrafast reflectivity and polarimetry probes to investigate carrier relaxation dynamics and ultrafast spin dynamics in Ni (111) single crystals, which serve as a typical model system for the study of magnetism owing to their partially filled 3d band electrons. Our experimental results indicate that, within the temporal resolution of our system, the electron and spin degrees of freedom indistinguishably respond to ultrafast deposition of laser pulse energies. However, the electron/lattice and spin/lattice couplings indicated different time scales, which is, to some extent, an interesting result because it is typically believed that the transfer of energy from the electron system is of the same order as the transfer of spin angular momentum to the lattice. However, one may need to integrate an ultrafast diffraction probe to further confirm those couplings with the lattice degree of freedom. This study may shine a light on the demand for integrating multiple ultrafast probes to explore couplings among electron, spin and lattice degrees of freedom in condensed matter.

2. Method

The experiments were performed on a homemade pump–probe system that integrates femtosecond optical reflectivity and polarimetry probes within the same time frame, namely, a precisely controllable and measurable timing between the reflectivity and polarimetry probes. A Ti:sapphire laser amplifier that operates at a 1 kHz repetition rate with a laser pulse duration of 35 fs and a central wavelength of 800 nm (1.55 eV) was used. The main pulse from the laser amplifier is split into pump and probe pulses whose optical path differences are precisely controlled by a mechanical stage. The probe pulse is converted to 400 nm (3.10 eV) by a second-harmonic crystal (a 0.2 mm thick beta barium borate crystal cut at $\theta = 29.2^\circ$ and $\phi = 0^\circ$ to provide type I phase matching), chopped with a frequency of 220 Hz and focused by a plano-convex lens onto the sample with a spot size of ~ 0.2 mm. The 400 nm probe pulse is focused on the sample with a spot size about five times smaller than the pump beam to ensure that the observed sample area is evenly excited. For ultrafast reflectivity measurements, the reflected probe pulse is directed to a photodiode through appropriate filters and attenuators in order to convert transient optical intensities at each delay time into electronic signals that are analyzed by a lock-in amplifier. For ultrafast polarimetry measurements, the probe pulse is directed to a Wollaston prism and a balanced photon detector to record the intensity changes of two different optical polarization directions. The signal-to-noise ratio of such measurements is optimized by combining a boxcar and lock-in amplifier. For both measurements, the angle between the pump and probe beam is smaller than 5° to achieve a nearly co-linear configuration. The Ni (111) single crystal is kept at room temperature on a sample holder. The thickness of the crystal is 500 μm. A static external magnetic field of 0.6 T is applied to the crystal as measured by a Hall sensor. For all experiments presented in this paper, the laser fluence was below the damage threshold of the sample, which remained intact when checked with an optical microscope after data acquisition.

3. Results and discussion

The carrier dynamics of Ni (111) single crystal were obtained by means of ultrafast reflectivity measurements and the data are depicted in Fig. 1. The change in optical intensity is described by the change of the output voltage from the photon detector and denoted as ΔR. Before recording any experimental data it was confirmed that the photon detector responds linearly with regard to the received probe light intensity. The time zero is defined by the onset of observable changes in reflectivity. Upon femtosecond laser excitation, the optical reflectivity rapidly reaches its extreme value, indicating the creation of a non-equilibrium state of electron carriers. Because the excitation photon energy of 1.55 eV is insufficient to create interband transitions, and the pump fluences in this study are also small enough, only electrons near the Fermi level are excited. Therefore, it is assumed that electrons mainly experience thermal excitation during photon absorption. According to the Drude model,[17] electrons within the optical penetration depth became energetic upon absorbing photons, and the optical reflectivity of the probe pulse generally changes rapidly within the first few hundred femtoseconds until it reaches the extreme value. The reflectivity follows a restoring process as the energies transfer from the electron subsystem to the spin and lattice degrees of freedom through electron–spin and electron–phonon couplings, as well as heat diffusion from within the skin depth to the specimen bulk. For five different pump energies, the trends are similar. To further confirm if the carrier relaxation dynamics are dominated by a single-particle process we normalized the reflectivity using its extreme value under each pump fluence and plotted the results as Fig. 1(b). It is clear that, under different pump fluences, the recovery follows almost the same characteristic time, which agrees with the Drude model assumed above, and

a single-particle relaxation mechanism is applicable.[17] It is worth mentioning that, around the hundreds of picoseconds time interval, the normalized signals exhibit a very small deviation from each other. This might indicate the slight existence of non-thermal effects;[18–20] however, the overall carrier relaxation dynamics are still dominated by the thermal relaxation mechanism, which is further confirmed by the linear plot of extreme values versus pump fluence in Fig. 1(c). Assuming that the carrier relaxation dynamics involve only electrons, the recovery rate can be obtained through exponential fitting to the experimental data, which indicates a time constant of 40 ps. This is a time scale that is larger than some previously reported values (this is probably because we employed a thick sample of $\sim$ 500 μm). Therefore, the measured reflectivity reflects not only the couplings between the electron subsystem with the spin and lattice subsystems that are mainly within the optical skin depth but also the diffusion of the deposited optical energy from the surface to the bulk of the crystal. The detailed dynamics of those two processes demand sophisticated numerical modeling. Here, we employed a bi-exponential fitting to obtain a preliminary insight. It delivers two characteristic times of $\sim$ 20 ps and $\sim$ 160 ps, which may correspond to the electron–phonon coupling and heat diffusion, respectively. It is also worth mentioning that, even for nanometer-think nickel crystals, the measured electron–phonon coupling time varies among different experimental techniques, possibly due to system deviations among *ex situ* measurements.[15,21–23] Therefore, this further indicates an urgent demand for the *in situ* integration of multiple ultrafast probes to establish a unified time frame and excitation conditions for the studies of couplings among different degrees of freedom. To further evaluate the couplings between the spin and lattice subsystems, we performed ultrafast polarimetry measurement using the same probing area of the sample and under the same pump conditions used in the ultrafast reflectivity experiments.

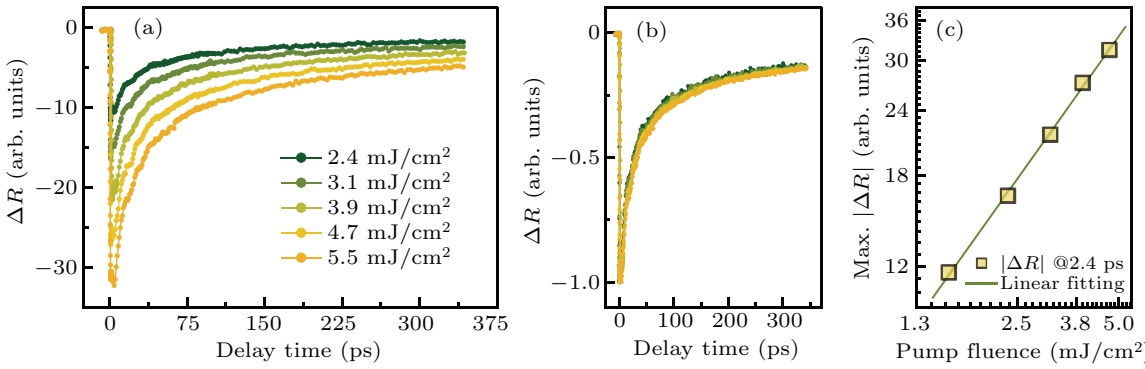


Fig. 1. Time-dependent reflectivity changes of Ni (111) single crystal after femtosecond laser excitation. (a) The reflectivity changes under five different pump fluences ranging from 2.4 mJ·cm^{-2} to 5.5 mJ·cm^{-2}. (b) The normalized reflectivity changes. For each pump fluence, the time-dependent reflectivity is normalized using the maximum change of reflectivity that appears around 2.4 ps after laser excitation. (c) A log–log plot depicting the maximum changes of reflectivity as a function of pump fluence; the slope is 0.92. The maximum reflectivity change is extracted from (a) on the left.

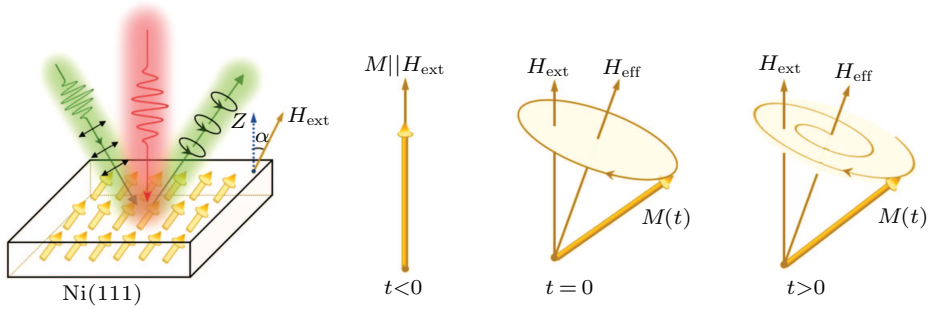


Fig. 2. Mechanism of ultrafast changes in magnetic momentum. (a) Configuration of the ultrafast polarimetry experiment. The S-polarized pump pulse perpendicularly impinges the nickel crystal, and the P-polarized probe pump is reflected by the sample with a small angle of 5° with respect to the pump beam. The polarization changes of the probe beam are recorded at each delay time for further analysis. The sample is uniformly situated in a static external magnetic field, $H_{\rm ext} = 0.6$ T, which is tilted by a small angle of $\alpha = 12°$ with respect to the normal direction, Z, of the crystal. (b) Illustration of the magnetic momentum before, at and after time zero. Transient changes in magnetic momentum due to pump laser pulses will result in a deviation of the magnetization direction from the external static field and a restoring process that exhibits precession of the spin angular momentum.

The ultrafast spin dynamics are revealed by the polarimetry probe, and the essential experimental configuration is demonstrated in Fig. 2. Before time zero, the ferromagnetic nickel crystal is fixed on a room-temperature sample holder and fully magnetized by an applied static external field of 0.6 T. However, upon excitation by the pump pulse, the rapid deposition of photon energy not only creates a nascent non-equilibrium state for the electrons and causes changes in op-

tical reflectivity but also affects the spin angular momentum of the electrons. Therefore, the total magnetic momentum of the optical-skin-depth area is no longer a saturated value determined by the applied external field but rather a time-dependent value associated with the non-equilibrium dynamics of the relaxation of spin angular momentum to other degrees of freedom. As reported in previous literature,[1] the laser-induced changes to the internal magnetic fields of the sample may be denoted as δH, and the total equivalent magnetic field is, therefore, a superposition of the applied static field H_{ext} and ΔM to create an effective magnetic field, H_{eff}, around which occurs spin precession and enables the internal magnetic momentum to restore to align with the applied external field. The relaxation of spin angular momentum is obtained by analyzing the time-dependent polarization change, as depicted in Fig. 3. Time zero is the same as that defined in the ultrafast reflectivity measurements. The magneto-optical signal exhibits a rapid drop within a femtosecond time interval due to the disturbance of the pump pulse. It is clear that the ultrafast polarimetry signal involves a damping oscillation that lasts over hundreds of picoseconds. For ultrafast polarimetry experiments, such oscillations are associated with the spin precessions after femtosecond demagnetization.[21] Here, we performed a fast Fourier transform and extracted a 28 GHz oscillation period. Given the applied field of 0.6 T, this is a reasonable value for ferromagnetic materials. We further performed pump fluence-dependent experiments; the results are summarized in Fig. 4. As the pump fluence increases, the oscillation amplitude of the polarimetry signal follows the same trend, but the period and damping rate remain unchanged. This indicates that the increased pump fluence introduces more considerable disturbance to the internal magnetic field. However, it does not alter the coupling rate between the spin and other degrees of freedom. The amplitude of the first three oscillations under each data set is plotted versus pump fluence and illustrated in Fig. 4(b). The log–log plot displays a linear relation with a slope of 1.1±0.2. Therefore, for all these measurements the photon-induced non-equilibrium dynamics remain in a linear region with respect to the pump fluence.

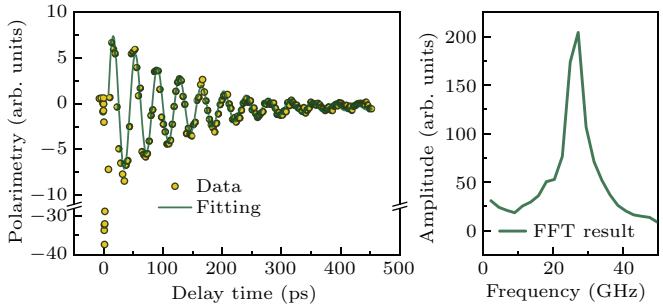


Fig. 3. The magneto-optical signal, recorded under 5.5 mJ·cm^{-2} pump fluence, depicted with its fast Fourier transform (FFT). The results indicate a precession frequency of 28 GHz for the magnetic momentum. The damping of the oscillation period is clearly observable, indicating a recovery of the total magnetic momentum.

It is interesting to compare the carrier dynamics with the spin dynamics obtained by the integrated ultrafast reflectivity and polarimetry probes. The precession of the magnetization is described by the Landau–Lifshitz–Gilbert equation,[24] and it is around the effective field, as has already been reported in various ferromagnetic materials. Such a precession follows the initial demagnetization of the Ni film induced by the excitation laser pulse, and it typically occurs within the thermalization time of the spins. Apparently, with increased pump fluence, a more significant demagnetization is desirable and eventually leads to a larger effective field. Therefore, the oscillation amplitudes shown in Fig. 4(a) scale with respect to the pump laser fluences. The log–log plots in Fig. 4(b) indicate a linear relation with a slope of 1.1±0.2. This suggests that the effective field scales linearly with excitation laser fluence. However, it is worth mentioning that according to the reflectivity signal obtained in our experiments there is no direct sign of acoustic phonons, which is observable in previous ultrafast diffraction experiments on nickel.[25] Integration of an ultrafast diffraction probe with optical probes may further benefit the measurement of couplings with the lattice degree of freedom.

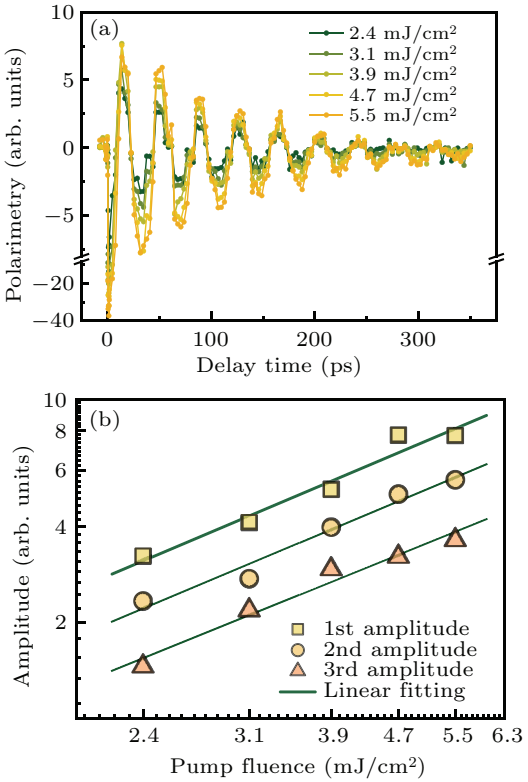


Fig. 4. The pump fluence-dependent precessions of the total magnetic momentum are presented with the amplitude of the first three oscillation periods. The linear fitting with the log–log plots also indicates a linear relation concerning the excitation laser fluences. The damping oscillations are characterized by a time constant of ∼ 120 ps, significantly larger than the electron relaxation time. This indicates that it took a long time for the spin degree of freedom to exchange energy with the electron and lattice subsystems, showing a much slower interaction with respect to electron–phonon coupling.

4. Conclusion

With ultrafast reflectivity and polarimetry probes, we have studied the relaxation of carrier dynamics and evolution of spin angular momentum in Ni (111) single crystal. Within the linear excitation fluences and the presence of a 0.6 T static magnetic field, the carrier relaxation time is tens of picoseconds; in contrast, restoring magnetic momentum takes about 120 ps. To further elucidate the deviation between the two time scales, characterization with ultrafast diffraction probes to further reveal the couplings between spin and lattice degrees of freedom may be needed.

Acknowledgements

Project supported by the National Key R&D Program of China (Grant Nos. 2022YFA1604402 and 2022YFA1604403), the National Natural Science Foundation of China (NSFC) (Grant No. 11721404), the Shanghai Rising-Star Program (Grant No. 21QA1406100), and the Technology Innovation Action Plan of the Science and Technology Commission of Shanghai Municipality (Grant No. 20JC1416000). Dr Rentzepis acknowledges support by the Air Force Office of Scientific Research (AFOSR) (Grant No. FA9550-20-1-0139) and the Texas A&M Engineering Experimental Station (TEES). Dr Li thanks the Shanghai Soft X-ray Free Electron Laser Project for providing the Ti:sapphire laser time to perform this study.

References

[1] Kirilyuk A, Kimel A V and Rasing T 2010 *Rev. Mod. Phys.* **82** 2731
[2] Tengdin P, You W, Chen C, Shi X, Zusin D, Zhang Y, Gentry G, Blonsky A, Keller M, Oppeneer P M, Kapteyn H C, Tao Z and Murnane M M 2018 *Sci. Adv.* **4** eaap9744
[3] Beaurepaire E, Merle J C, Daunois A and Bigot J Y 1996 *Phys. Rev. Lett.* **76** 4250
[4] van Hees Y L W, Koopmans B and Lavrijsen R 2022 *Appl. Phys. Lett.* **120** 252401
[5] Dornes C, Acremann y, Savoini M, Kubli M, Neugebauer M J, Abreu E, Huber L, Lantz G, Vaz C A F, Lemke H, Bothschafter E M, Porer M, Esposito V, Rettig L, Buzzi M, Alberca A, Windsor Y W, Beaud P, Staub U, Zhu D, Song S, Glownia J M and Johnson S L 2019 *Nature* **565** 209
[6] Güdde J, Conrad U, Jähnke V, Hohlfeld J and Matthias E 1999 *Phys. Rev. B* **59** R6608(R)
[7] Tian Y C, Zhang W H, Li F S, Wu Y L, Wu Q, Sun F, Zhou G Y, Wang L, Ma X, Xue Q K and Zhao J 2016 *Phys. Rev. Lett.* **116** 107001
[8] Hu L L, Yang M, Wu Y L, Wu Q, Zhao H, Sun F, Wang W, He R, He S L, Zhang H, Huang R J, Li L F, Shi Y G and Zhao J 2019 *Phys. Rev. B* **99** 094307
[9] Wu Q, Zhou H, Wu Y, Hu L, Ni S, Tian Y, Sun F, Zhou F, Dong X, Zhao Z and Zhao J 2020 *Chin. Phys. Lett.* **37** 097802
[10] Sheu Y M, Chang Y M, Chang C P, Li Y H, Babu K R, Guo G Y, Kurumaji T and Tokura Y 2019 *Phys. Rev. X* **9** 031038
[11] Afanasiev D, Hortensius J R, Ivanov B A, Sasani A, Bousquet E, Blanter Y M, Mikhaylovskiy R V, Kimel A V and Caviglia A D 2021 *Nat. Mater.* **20** 607
[12] Hortensius J R, Afanasiev D, Matthiesen M, Leenders R, Citro R, Kimel A V, Mikhaylovskiy R V, Ivanov B A and Caviglia A D 2021 *Nat. Phys.* **17** 489
[13] van Kampen M, Jozsa C, Kohlhepp J T, LeClair P, Lagae L, de Jonge W J M and Koopmans B 2002 *Phys. Rev. Lett.* **88** 227201
[14] Sun F, Zhang T, Yi C J, Wu Y L, Zhao H, Wu Q, Shi Y G, Weng H and Zhao J 2021 *Phys. Rev. B* **104** L100301
[15] Tauchert S R, Volkov M, Ehberger D, Kazenwadel D, Evers M, Lange H, Donges A, Book A, Kreuzpaintner W, Nowak U and Baum P 2022 *Nature* **602** 73
[16] Zong A, Zhang Q, Zhou F, Su Y, Hwangbo K, Shen X, Jiang Q, Liu H, Gage T E, Walko D A, Kozina M E, Luo D, Reid A H, Yang J, Park S, Lapidus S H, Chu J H, Arslan I, Wang X, Xiao D, Xu X, Gedik N and Wen H 2023 *Nature* **620** 988
[17] Smith A N and Norris P M 2001 *Appl. Phys. Lett.* **78** 1240
[18] de la Torre A, Kennes D M, Claassen M, Gerber S, McIver J W and Sentef M A 2021 *Rev. Mod. Phys.* **93** 041002
[19] Windsor Y W, Zahn D, Kamrla R, Feldl J, Seiler H, Chiang C T, Ramsteiner M, Widdra W, Ernstorfer R and Rettig L 2021 *Phys. Rev. Lett.* **126** 147202
[20] Giri A and Hopkins P E 2015 *J. Appl. Phys.* **118** 215101
[21] Kim J W, Vomir M and Bigot J Y 2012 *Phys. Rev. Lett.* **109** 166601
[22] Wang X, Nie S, Li J, Clinite R, Clark J E and Cao J 2010 *Phys. Rev. B* **81** 220301
[23] van Kampen M, Kohlhepp J T, de Jonge W J M, Koopmans B and Coehoorn R 2005 *J. Phys.: Condens. Matter* **17** 6823
[24] Gilbert T L 2004 *IEEE Transactions on Magnetics* **40** 3443
[25] Li R, Elsayed-Ali H E, Chen J, Dhankhar D, Krishnamoorthi A and Rentzepis P M 2019 *The Journal of Chemical Physics* **151** 124702